Journal of Power Sources 251 (2014) 476–479

Contents lists available at ScienceDirect

Journal of Power Sources

journal homepage: www.elsevier.com/locate/jpowsour

Short communication

Analysis of integrated electrode stacks for lithium ion batteries

Michael L. Lazar [a], Ben Sloan [b], Steven Carlson [b], Brett L. Lucht [a,*]

[a] University of Rhode Island, Kingston, RI 02881, USA
[b] Optodot Corporation, 2 Kingsbury Ave, Watertown, MA, USA

HIGHLIGHTS

- A process to prepare novel stacked electrodes for lithium ion batteries was developed.
- Coin cells were prepared and cycled with novel stacked anodes and cathodes.
- Cells with novel stacked electrodes had similar cycling performance to traditionally prepared lithium ion cells.
- SEM images suggest that the novel stacked electrodes have good stability after cycling.

ARTICLE INFO

Article history:
Received 5 September 2013
Received in revised form
6 November 2013
Accepted 21 November 2013
Available online 1 December 2013

Keywords:
Lithium ion batteries
Electrodes
Integrated cells
Volumetric energy density

ABSTRACT

In an effort to reduce the cost of manufacturing lithium ion batteries, a novel approach is being developed to build a one piece integrated cell via layer by layer coating deposition rather than manufacturing separate pieces followed by electrode stacking and assembly. This new process would hold several advantages by providing excellent contact and thinner deposits, which will conserve space for energy storing materials while reducing production costs. Anode and cathode half stacks are made using a new process and the electrodes have been investigated in coin cells. Each half stack consists of a current collector, electrode, and separator combined into a single component. The stack cells successfully cycle as graphite stack/lithium and $LiNi_{1/3}Mn_{1/3}Co_{1/3}O_2$/lithium cells and together in graphite stack/$LiNi_{1/3}Mn_{1/3}Co_{1/3}O_2$ stack cell arrangements. Cross sectional SEM images show very little change in the anode and cathode materials indicating that the material is stable under typical cycling conditions and at moderately elevated temperature (55 °C). While the electrode stacks investigated are not optimized, the results support good cycling performance for a stacked cell design.

© 2013 Elsevier B.V. All rights reserved.

1. Introduction

Improvement of the cell design of lithium ion batteries is important to lowering manufacturing costs, which is one of the major hurdles for the widespread implementation of lithium ion batteries into electric vehicles [1]. A novel approach to lowering the manufacturing cost of lithium ion batteries is to build cells via a layer by layer coating deposition process as opposed to the current preparation via slurry coated electrodes and free-standing separators which are then assembled via stacking or winding. The layer by layer method can further benefit cells by providing thinner layers, which have the potential to conserve space, improve the volumetric energy density, and decrease the quantity of inactive components (separator, current collectors, and electrolyte) and thus the cost of the materials within the cell. This process also has the potential for battery preparation via layering electrodes in a single manufacturing process, allowing most of the work to be accomplished through automation reducing the coating and assembly cost. The concept of a cell stack has been investigated but there are few reports in the literature [2–5]. Most of the research in this area has focused on the development of novel separators rather than developing an electrode stack [6]. These investigations focused on polymer separators with ceramic additives [2–4,7,8], or developing separators consisting of ceramic and binder [5]. Since the idea of a stacked cell has not been significantly studied or optimized, the goal of this research was to develop a method to prepare a cell stack with comparable performance to traditional cells.

2. Experimental

2.1. Preparation of the electrodes

Anode stacks are composed of approximately 13 μm of separator, 43 μm of graphite anode and 11 μm of copper. The cathode

* Corresponding author. Tel.: +1 401 874 5071; fax: +1 401 874 5072.
E-mail address: blucht@chm.uri.edu (B.L. Lucht).

0378-7753/$ – see front matter © 2013 Elsevier B.V. All rights reserved.
http://dx.doi.org/10.1016/j.jpowsour.2013.11.065

stacks are composed of approximately 10 μm of separator, 73 μm of $LiNi_{1/3}Mn_{1/3}Co_{1/3}O_2$ (NMC) cathode and 11 μm of aluminum. Each stack is layered into one bonded and inseparable piece rather than existing as separate pieces of metal/electrode and separator as in the current manufacturing process for cells. The graphite anodes and NMC cathodes (92% active material along with PVDF binder and conductive carbon) were coated directly onto the ceramic separator layer. This is afforded by the small pores of the ceramic separator (30 nm diameter) which prevent penetration of the electrode materials into the separator layer.

The anode stacks were made by first coating a separator layer of aluminum boehmite and polymer onto a silicone-treated polyester release film. The porosity of the separator layer was approximately 43%. The average pore size diameter of the separator layer was approximately 30 nm with a very narrow pore size distribution. Next, a commercial graphite anode layer was coated onto the separator layer. Then, the copper layer was sputtered onto the anode layer, followed by delamination of the release substrate to provide the anode stack. The cathode stacks were made similarly by coating a commercial NMC cathode onto the separator layer on the release film and then sputtering an aluminum layer onto the cathode layer. Delaminating the release film provided the cathode stack.

2.2. Assembly of the coin cells and cycling

Each sample was evaluated in a coin cell versus lithium metal. The electrode stacks were cut to a diameter of 14.7 mm and assembled in a coin cell using 40 μL of electrolyte (1 M $LiPF_6$ in 1:1:1 ethylene carbonate/dimethyl carbonate/diethyl carbonate (EC/DMC/DEC) [9]) and a protective polyolefin separator ring with an inner diameter of 12 mm and an outer diameter of 19 mm. The separator, which is about 10 μm thick, is only large enough to cover the electrode, a polyolefin ring was used to prevent possible shorting at the edges of the electrode due to the presence of loose particles resulting from electrode cutting and may contact the lithium electrode and result in shorting.

Both the Li/graphite and Li/NMC cells were initially cycled at a C/20 rate for five cycles followed by five C/10 cycles, ten C/5 cycles, ten C/2 cycles, and three C/20 cycles. The total capacity of each Li/graphite composite cell was about 3.4 mAh and the total capacity of each Li/NMC composite cell was about 4.2 mAh. Additionally, graphite/NMC cells were prepared with a 15 mm diameter graphite/separator stack and a 12.7 mm diameter NMC/separator stack. The theoretical capacity of the cell is 3.1 mAh and is cathode limited. The cells were cycled with the same profile as discussed above. The full cells also contain the protective polyolefin ring used in the half cells to prevent shorting from the edges of the electrodes. Fig. 1 depicts the configuration of the graphite stack/NMC stack cell.

Additionally, full cells were prepared and cycled at 55 °C to simulate accelerated aging. The cells were full cells constructed as above and used 30 μL of electrolyte. The formation cycling was one cycle at C/20 followed by two cycles at C/10 and two cycles at C/5 rates. The cells were then cycled at a C/5 rate for ten cycles at 16 °C, ten cycles at 55 °C and ten cycles at 16 °C.

2.3. Preparation for SEM

The electrode stacks were imaged using cross sectional SEM with fresh electrode stacks and electrode stacks cycled in graphite/NMC cells. The fresh samples were prepared by cutting a piece of a small part of the electrode with a razor blade with the separator side facing the blade. Cycled cells were opened in an argon filled glove box, rinsed three times with dimethyl carbonate, and vacuum dried overnight to remove the excess DMC then cut with a razor blade.

3. Results

3.1. Cycling of Li/graphite stack and Li/NMC stack cells

The cycling efficiencies of the Li/graphite stack cells during the initial formation cycles are lower (40–80%) than is typically observed for Li/graphite cells (70–80%). However, after the formation cycles (first five cycles) the cycling efficiency is very good, >99% (Fig. 2). Much better first cycle efficiency (~85%) is observed for graphite stack/NMC stack cells, as discussed below. Thus, the low efficiency during formation cycling may result from detrimental interactions between the lithium metal and the edges of the cut electrode stack. The capacity drops significantly for Li/graphite cells with increased cycling rates. Only ~30 mAh (~10% of the initial capacity) is obtained from cells cycled at C/2. However, the capacity lost upon cycling at high rate can be recovered with low rate cycling consistent with slow kinetics as opposed to irreversible capacity loss. Despite the poor rate performance, the efficiency of the Li/graphite cells is very good at all rates (>99%). The Li/NMC stack cells have good first cycle efficiency (85–90%) and discharge capacity (145 mAh g^{-1}). Upon cycling at higher rates the Li/NMC stack cells retain good efficiency (>95%) and discharge capacity at C/10 and C/5, but the capacity drops off at higher rate (C/2, Fig. 3). In general, both the Li/graphite stack and Li/NMC stack cells have satisfactory performance. Thus, graphite stack/NMC stack cells were prepared and investigated.

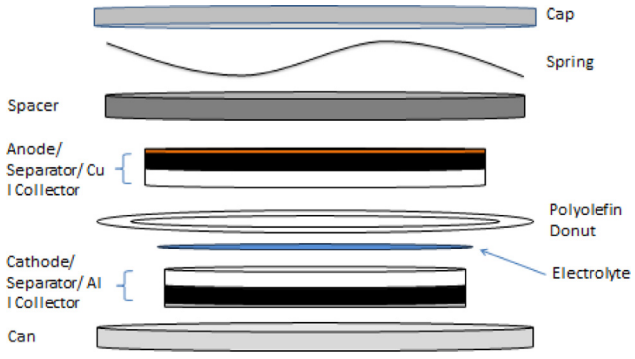

Fig. 1. Schematic of a graphite stack/NMC stack cell.

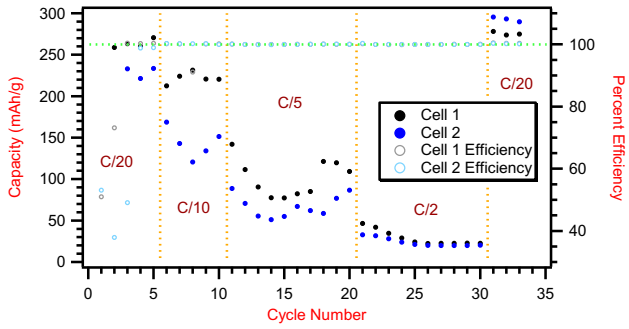

Fig. 2. Graphite stack/lithium cell discharge capacity at various rates along with cycling efficiency.

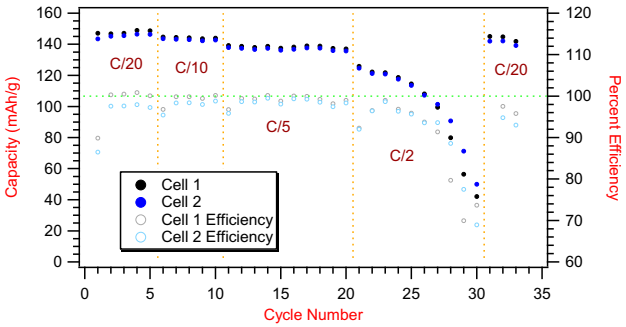

Fig. 3. NMC stack/lithium cell discharge capacity at various rates along with cycling efficiency.

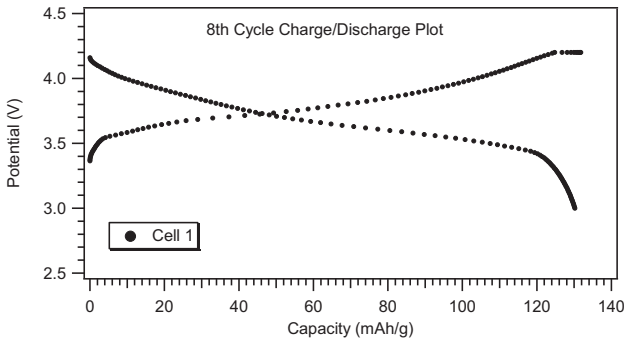

Fig. 5. Eighth cycle charge and discharge plots of a graphite stack/NMC stack cell.

3.2. Graphite stack/NMC stack cells

Graphite stack/NMC stack cells were prepared and cycled (Fig. 4). The first cycle efficiency is 85% and the discharge capacity is 150 mAh g^{-1}. The irreversible capacity on the first cycle is consistent with the formation of a solid electrolyte interface (SEI) on the graphitic anode [10]. The cells retain high capacity as the cycling rate is increased from C/20 to C/2. The cells still deliver 120 mAh g^{-1} at the fastest rate (C/2) and the cycling efficiency is high for all cells, >98%. After cycling at high rate, the cells are able to deliver >90% of the initial capacity at C/20 (140 mAh g^{-1}) suggesting that the cells have stable cycling performance. The cycling performance is comparable to standard graphite/NMC cells prepared with traditional polyolefin separators [11].

The charge–discharge plot of the eighth cycle is provided in Fig. 5. The charge and discharge plots are symmetrical with a small hysteresis, and are typical for graphite/NMC cells further supporting comparable performance of the graphite/separator stack and NMC/separator stack electrodes to traditional coated electrodes with polyolefin separators.

3.3. Elevated temperature cycling

Additional graphite stack/NMC stack cells were cycled at 55 °C to simulate accelerated aging (Fig. 6). The cells cycled well, with only an 8% capacity loss during the ten cycles at 55 °C. Upon returning the cells to 16 °C after cycling at 55 °C, the cells retained 88% of the initial RT capacity. The good cycling stability at elevated temperature can be attributed to the good thermal stability of the separator and the Lewis basic nature of the aluminum boehmite [12]. The cycling performance of the first generation electrode separator stacks suggests that separated coated electrode stacks may be a viable option for the next generation of lithium ion batteries. To better understand the structure of the electrode stacks before and after cycling at 16 °C and 55 °C, cross sectional SEM images of the electrodes were obtained.

3.4. SEM Imaging of electrodes

SEM cross sectional images of the graphite separator stack and the cathode separator stack, both fresh and after cycling, are provided in Fig. 7. For the anode images, the copper is the bright material at the top of the image and is approximately 11 μm thick. The dark material in the center of the image is the active graphite anode material and has a thickness of 40–45 μm and the separator is the smooth light colored material at the bottom of the image with a thickness around 13 μm. The top of the anode stack has a significant undulation due to variations in the thickness of the active graphite layer which is likely due to a lack of calendaring of the samples. After cycling the top surface is somewhat smoother, presumably due to the stack pressure within the cell. Otherwise, there are no significant changes to the electrode materials suggesting that the graphite stack anode is stable upon cycling.

The cathode stack is more uniform than the anode stack. The top bright layer is the sputtered aluminum. The aluminum layer is approximately 11 μm thick but it is difficult to distinguish due to the similarity of brightness to the cathode material. However, the aluminum aggregates are smoother and smaller particles than the active metal oxide. The active NMC layer is in the center and is 70–75 μm thick and the separator is the smooth layer at the bottom of the image and is about 10 μm thick. The separator has some bright spots due to charge build up during imaging. The cross sectional SEM images for the cycled cathode stacks do not differ significantly from the images of the fresh cathode stacks which indicate that the cathode is stable to cycling.

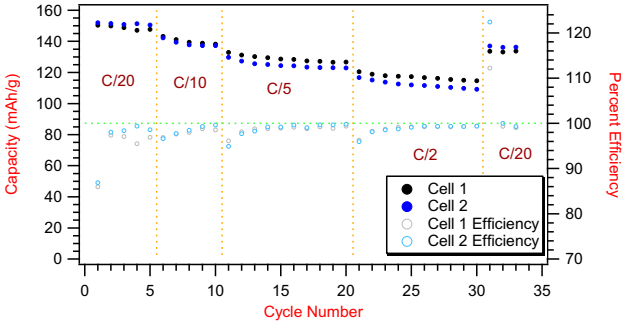

Fig. 4. Graphite stack/NMC stack cell discharge plot at various rates along with cycling efficiency.

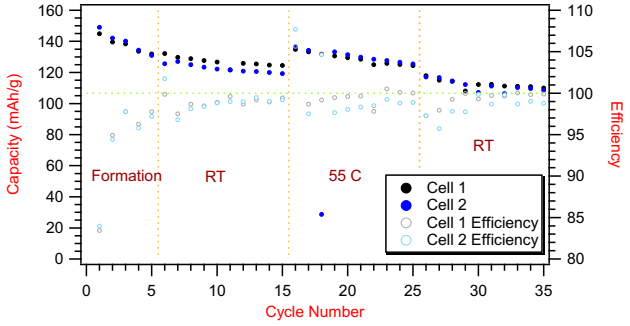

Fig. 6. The efficiency and discharge capacity of a graphite stack/NMC stack cell cycled at 16 °C (RT), 55 °C, and 16 °C (RT), at a C/5 rate.

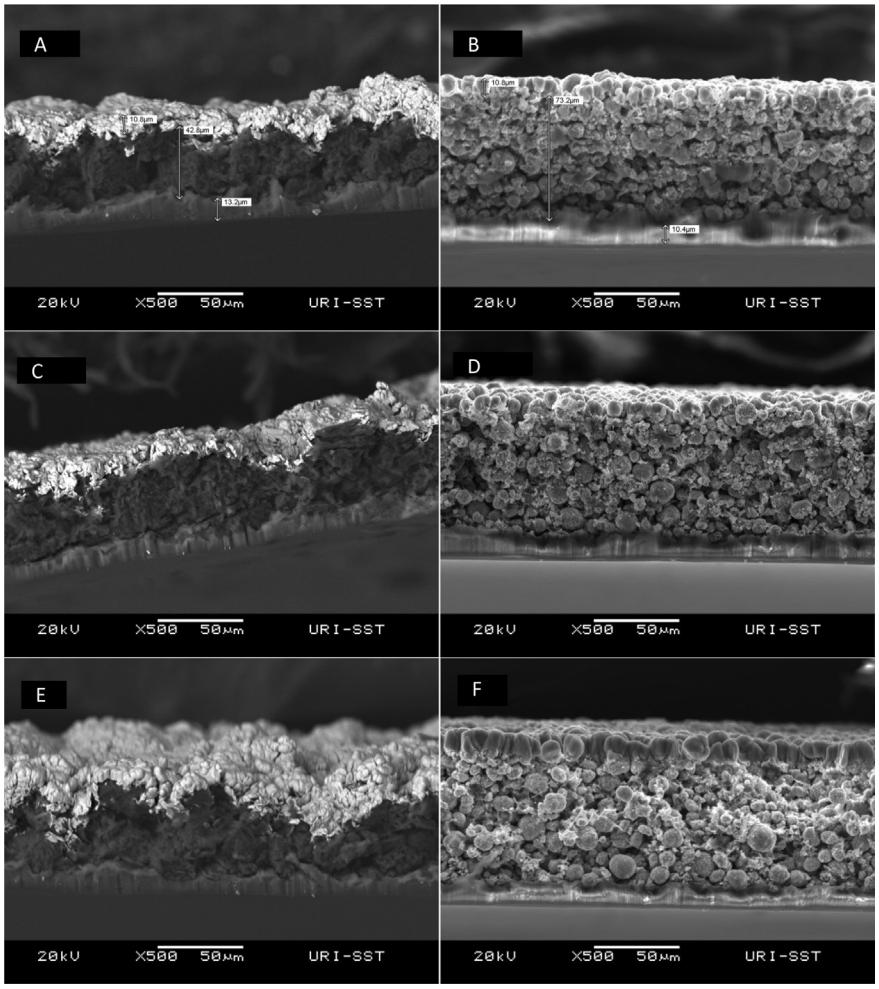

Fig. 7. Cross sectional SEM images of: A) Fresh graphite stack. B) Fresh NMC stack. C) Cycled graphite stack. D) Cycled NMC stack. E) Graphite stack after cycling at 55 °C. F) NMC stack after cycling at 55 °C. The graphite stack samples were taken using backscatter electron imaging and the NMC stack samples were taken using secondary electrons imaging. All samples were taken at 20 kV under high vacuum and each image from top to bottom is the current collector, the active material, and the separator.

SEM images of the electrodes after cycling at 55 °C are provided in Fig. 7, images E and F. The images are similar to the images of the fresh electrodes and electrodes extracted from cells cycled at 16 °C. There is no evidence of damage to either the graphite stack electrode or the NMC stack electrode.

4. Conclusion

Layered electrode stacks were prepared with copper/graphite/separator and aluminum/NMC/separator. The layered electrode stacks were cycled with lithium metal anodes. The Li/graphite stack cells have poor first cycle efficiency, but have high discharge capacity after the first cycle ~250 mAh g^{-1}. The Li/NMC stack cells have good first cycle efficiency and reasonable discharge capacity (145 mAh g^{-1}) and good rate performance up to C/5. However, the graphite stack/NMC stack cells have the best performance. The cells have high first cycle reversibility (85%), good capacity (150 mAh g^{-1}) and good rate performance up to C/2. These cells also cycle well at 55 °C consistent with good calendar life performance. Ex-situ analysis of the electrode stacks before and after cycling suggest that cycling does not induce significant changes to the electrode stack structure and is consistent with good cycling behavior, even at 55 °C. The results suggest that the use of layered stack electrodes is a promising alternative for the preparation of lithium ion batteries.

Acknowledgment

Special thanks for the funding of this project go to Optodot and the U.S. Department of Energy grant number DE-EE0005433.

References

[1] J.B. Goodenough, Acc. Chem. Res. 46 (2013) 1053.
[2] J.M. Tarascon., A.S. Gozdz, C. Schmutz, F. Shokoohi, P.C. Warren, Solid State Ionics 86-88 (1996) 49–54.
[3] R.A.M. Hikmet, J. Power Sources 92 (2001) 212–220.
[4] P.P. Prosini, P. Villano, M. Carewska, Electrochem. Acta 48 (2002) 227–233.
[5] J. Chen, H. Xiang, Zhang, L.H. Wang, J. Appl. Electrochem. 42 (2012) 471–475.
[6] S.S. Zhang, J. Power Sources 164 (2007) 351–364.
[7] A. Du Pasquier, P.C. Warren, D. Culver, A.S. Gozdz, G.G. Amatucci, J.M. Tarascon, Solid State Ionics 135 (2000) 249–257.
[8] W.-K. Shin, D.-W. Kim, J. Power Sources 226 (2013) 54–60.
[9] M.C. Smart, B.V. Ratnakumar, S.J. Surampudi, Electrochem. Soc. 146 (1999) 486.
[10] M. Nie, D. Chalasani, D.P. Abraham, Y. Chen, A. Bose, B.L. Lucht, J. Phys. Chem. C 117 (3) (2013) 1257–1267.
[11] I. Bloom, L.K. Walker, J.K. Basco, D.P. Abraham, J.P. Christopherson, C.D. Ho, J. Power Sources 195 (2010) 877–882.
[12] W. Li, C. Campion, B.L. Lucht, B. Ravdel, K.M. Abraham, J. Electrochem. Soc. 152 (2005) A1361.